Chemico-Biological Interactions 416 (2025) 111531

Contents lists available at ScienceDirect

Chemico-Biological Interactions

journal homepage: www.elsevier.com/locate/chembioint

Research paper

Transcriptome profiling and DNA methylation analysis of human hepatocyte cell line HHL-16 in response to aflatoxin B1

Hang Wu [a,b], Yun Yun Gong [b], John Huntriss [a], Michael N. Routledge [c,d,*]

[a] School of Medicine, University of Leeds, Leeds, LS2 9JT, UK
[b] School of Food Science and Nutrition, University of Leeds, Leeds, LS2 9JT, UK
[c] Leicester Medical School, University of Leicester, Leicester, LE1 7RH, UK
[d] School of Food and Biological Engineering, Jiangsu University, Zhenjiang, 212013, China

ARTICLE INFO

Keywords:
Aflatoxin B1
HHL-16 cells
Gene expression
Pathways
DNA methylation

ABSTRACT

Dietary exposure to aflatoxin B1 (AFB1) can cause acute aflatoxicosis and liver cancer, and is associated with immune suppression and growth impairment, but the molecular mechanisms of the health effects are not fully understood. A non-neoplastic human hepatocyte cell line 16 (HHL-16) was utilized to understand the effects of AFB1 on transcriptome and DNA methylation changes, identifying molecular pathways underlying toxicity and health effects. RNA sequencing and bioinformatic analysis (RNA-Seq) was applied to find the genes and pathways affected by AFB1. Bisulfite pyrosequencing was used to assess DNA methylation levels of CpG sites around promoter regions of gene of interest. RNA-sequencing revealed 280 significantly up-regulated and 296 significantly down-regulated genes in HHL-16 cells after 20 μg/ml AFB1 treatment for 24 h. KEGG pathway enrichment analysis indicated that differentially expressed genes (DEGs) were significantly enriched in the following pathways: cytokine-cytokine receptor interaction, NF-kappa B signalling pathway, TNF signalling pathway, IL-17 signalling pathway, amoebiasis, MAPK signalling pathway, and lipid and atherosclerosis. Further DNA methylation analysis found that there was significant hypomethylation at one CpG site of *CCL20* after 20 μg/ml AFB1 treatment on HHL-16 cells for 24 h. In conclusion, AFB1 modulates the expression of genes related to the pathways that play important roles in inflammatory response, growth, and cancers, and demonstrates the effects of AFB1 on DNA methylation.

1. Introduction

Aflatoxins are the most poisonous mycotoxin produced by *Aspergillus flavus* and *A. parasiticus*, commonly contaminating various foods in tropical and subtropical regions, causing great health concerns in low-income countries, particularly in sub-Saharan Africa and South Asia [1]. Four major types of aflatoxins are aflatoxin B1 (AFB1), aflatoxin B2 (AFB2), aflatoxin G1 (AFG1) and aflatoxin G2 (AFG2), named because of their blue (B) and yellow green (G) fluorescence emitted under UV light [2]. Two hydroxylated metabolites of AFB1 and AFB2, aflatoxin M1 (AFM1) and aflatoxin M2 (AFM2) respectively, are commonly found in milk and dairy products [3]. AFB1 is the most prevalent, and most toxic form, which has been classified as a Group 1 carcinogen to humans by the International Agency for Research on Cancer (IARC) [4]. Dietary exposure to AFB1 has been reported to cause acute aflatoxicosis and liver cancer, and be associated with immune suppression and growth retardation [5].

Aflatoxin exposure has both acute and chronic effects on human health, which is a heavy burden on public health in low-income or middle low-income populations in tropical areas, due to the high susceptibility of foods to aflatoxin contamination in those regions and reliance on a contaminated staple food. High levels of aflatoxin exposure in a short time cause acute aflatoxicosis, which has been reported several times in Africa. For instance, 20 patients admitted to hospital with a case fatality rate of 60 % because of acute aflatoxicosis was reported in Machakos district of Kenya from March to June 1981 [6]. Another larger outbreak of aflatoxin poisoning in Kenya during January–June 2004 showed 317 patients with hepatic injury admitted to hospital, of which 125 cases died due to acute aflatoxicosis [7]. However, chronic effects of aflatoxin exposure due to low concentration over a long period of time is more commonly seen. The best documented chronic health effect of aflatoxin exposure is hepatocellular carcinoma (HCC) [8], and the

* Corresponding author. Leicester Medical School, University of Leicester, Leicester, LE1 7RH, UK.
E-mail address: mnr9@leicester.ac.uk (M.N. Routledge).

https://doi.org/10.1016/j.cbi.2025.111531
Received 6 November 2024; Received in revised form 27 January 2025; Accepted 25 April 2025
Available online 25 April 2025
0009-2797/© 2025 The Authors. Published by Elsevier B.V. This is an open access article under the CC BY-NC-ND license (http://creativecommons.org/licenses/by-nc-nd/4.0/).

broader effects including immune suppression and child growth impairment associated with aflatoxin exposure have also been reported [9,10].

The molecular mechanism of aflatoxin-induced hepatocarcinoma is the most well-established, with a hotspot mutation at codon 249 of p53, being strongly associated with dietary aflatoxin intake [11,12], and the DNA adduct formed by AFB1 exposure causing G to T transversions, consistent with the mutation pattern seen in human liver tumors [13–15].

The mechanism of aflatoxin exposure related immune suppression and growth impairment is not fully understood. However, current state of knowledge proposes that aflatoxin exerts effects on immune system through the disruption of innate immunity, cellular-mediated immunity, and humoral immunity. Decreased natural killer cell function in mice, and compromised phagocytic activity in chickens have been observed after aflatoxin feeding [16,17]. There are inconsistent findings of the effects of aflatoxin on humoral immunity, and major studies were investigated in poultry [18,19]. In cellular-mediated immunity, Zimmermann et al. conducted MTT assay in broiler lymphocytes treated with different concentrations of AFB1, and found that 10 μg/ml AFB1 treatment at 48 h, and 10 and 20 μg/ml AFB1 treatments at 72 h significantly decreased the cell viability of lymphocytes [20]. In addition, interference of cytokines production by lymphocytes and macrophages could affect all kinds of immune response directly or indirectly, but the changes in cytokines production, such as TNF-α and IL-6, caused by aflatoxin show a high variability. The inconsistent and inconclusive evidence mentioned above could be because of species variation of animal and cell lines, as well as treatment concentrations and timepoints of aflatoxin. Due to the conflicting results in the literature, the effects of aflatoxin exposure on the immune system still needs further investigation.

Recently, there is rapidly increasing interest in the mechanism of aflatoxin-associated child growth impairment [21,22]. Suggested explanations of potential mechanisms for aflatoxin-associated child growth impairment may include: contribution to enteropathy, immune suppression and/or changes in insulin-like growth factor (IGF) axis via liver toxicity [23]. After exposure to a combination of AFB1 and AFM1, intestinal barrier dysfunction in ICR mice and reduced intestinal integrity and permeability in Caco-2 cell line were observed, so aflatoxin exposure related intestinal damage may affect nutrition absorption and subsequent growth [24]. It was also postulated that the immunosuppressive effects of aflatoxin might increase infection risk to various diseases, for example, HIV, diarrhoea, and possibly compromised vaccine efficacy, which might suppress appetite and impair nutrition absorption [23].

The possibility that changes to the IGF axis may be involved, in the effects of aflatoxin exposure on child growth has been investigated. Two cohort studies carried out in Kenyan schoolchildren and Gambian infants found that there was negative association between aflatoxin exposure levels and the protein levels of growth factors IGFBP3 [25,26]. Additionally, differential DNA methylation of CpG sites in growth factor genes and immune-related genes has been reported in the children exposed to aflatoxin *in utero* [27]. To date, the findings of aflatoxin-associated DNA methylation and altered protein expression in the studies may shed light on aflatoxin-associated impaired child growth, however, a consistent alteration of specific genes affected by aflatoxin exposure has not been determined.

With the recent development of deep-sequencing technologies, the accessibility of RNA-Seq has been applied to transcriptome profiling. Understanding of the transcriptome helps to find the functional elements of the genome and figure out the molecular mechanisms of development and disease [28]. RNA-Seq has been used to assess the effects of aflatoxin on transcriptome changes in various animals and *in vitro* studies [29–32]. For example, hepatic transcriptome changes in ducklings administrated with AFB1 showed that differentially expressed genes (DEGs) involved in phase I metabolism, phase II detoxification, carcinogenesis, and fatty acid metabolism [29]. However, there are some inconsistencies of the enriched pathways found in different animals or cell lines, and more evidence of transcriptome changes caused by aflatoxin is required. Moreover, most of the current evidence of the effects of aflatoxin on transcriptome profile in cell lines are based on cancer-derived cells. Systematic measurement of gene expression in non-cancer cells treated with AFB1 has not been explored. Therefore, in this study, RNA-Seq method was used to analyse the alteration of hepatic transcriptome in HHL-16 cells (non-cancer cells) after AFB1 treatment, which will provide a better understanding and more evidence of aflatoxin-induced health effects.

2. Materials and methods

2.1. Cell maintenance and AFB1 treatments

Human hepatocyte line 16 (HHL-16), a non-tumorigenic human liver cell line, was kindly provided by Dr. Arvind H. Patel (MRC Virology Unit, Glasgow) [33]. HHL-16 cells were cultured in Gibco Minimum Essentia Media (MEM) supplemented with 10 % foetal bovine serum (FBS) and 1 % penicillin-streptomycin. The cells were grown in an incubator at 37 °C with a humidified atmosphere and 5 % CO2 supplied. The cells were passaged every 2 or 3 days when the cell confluency reaches up to 80 %. Passage 20–30 were used for all cell experiments.

AFB1 powder was dissolved in sterile-filtered DMSO to form a stock concentration of 20 mg/ml, and the final concentrations of AFB1 used in other experiments were diluted with cell culture medium. The cells were treated with 20 μg/ml AFB1, and its control treatment, 1:1000 diluted DMSO for 24 h, which is equivalent to the concentration in 20 μg/ml AFB1 treatment. Each treatment had three technical repeats, i.e., three wells with the same treatment in a 6-well plate. In addition, three biological repeats were performed.

2.2. RNA extraction

After incubation for the designated time, HHL-16 cells were harvested to extract total RNA using ReliaPrepTM RNA Cell Miniprep Kit. Briefly, after treatment with various concentrations, to collect the cells, the previous media containing AFB1 were aspirated, and the cells were washed with PBS. Then the cells were trypsinized for 5 min, and new media containing FBS was added to stop the trypsinization. The cell pellet was collected after centrifuge and the supernatant was aspirated out prior to the collection.

After harvest of the cells, total RNA from the cells were extracted by using ReliaPrepTM RNA Cell Miniprep Kit, and procedures are followed by the manufacturer's instructions. According to the cell number, an appropriate volume of BL + TG buffer (kit provided) was added into the tubes containing cell pellets, then 100 % isopropanol was added, followed by vortexing. The lysate was transferred to a spin ReliaPrepTM Minicolumn placed in a collection tube and centrifuged at 12000 g for 1 min at room temperature. The liquid in the collection tubes was discarded and the ReliaPrepTM Minicolumn was washed with RNA Wash Solution and centrifuged at 12000 g for 1 min. Then DNase I incubation procedure was performed. A mix of 24 μl Yellow Core Buffer, 3 μl 0.09 M MnCl2, and 3 μl DNase I enzyme was prepared and added into the ReliaPrepTM Minicolumn membrane for each sample. After incubating the DNase I Mix at room temperature for 15 min, Column Wash Solution was added into the column and centrifuged as before. Followed by two times of addition of RNA Wash Solution and centrifuge at 12000 g for 1 min. The wash solutions were discarded and after centrifuge at the full speed for 2 min, the ReliaPrepTM Minicolumn was placed into a new 1.5 ml RNase-free microtube. 30–50 μl RNase-free water was added into the membrane to elute RNA. After a centrifuge, the RNA samples were collected and tested by NanoDrop ND-100 Spectrophotometer. Purified RNA samples were directly used for reverse transcription or stored in −80 °C freezer for future use. The RNA samples were shipped with dry

ice to Novogene Co., Ltd for RNA-Sequencing.

2.3. RNA-Seq

RNA-Sequencing was performed in Novogene Co., Ltd through Illumina platforms, which is based on a paired-end 150 bp sequencing strategy, and it was followed with the steps including sample quality control, library construction, library quality control, sequencing, data quality control, and bioinformatics analysis.

With respect to sample quality control, concentrations and quality of the RNA, samples were tested by Agilent 5400. Only the samples meeting the requirement of both amount and quality were used for sequencing, which requires the amount of RNA samples to be at least over 200 ng and the RNA Integrity Number (RIN) to be at least over 4 (scale from 1 to 10, 10 is the best quality).

To get purified messenger RNA (mRNA), Poly-T oligo-attached magnetic beads were used in the total RNA samples to capture Poly-A enriched mRNA. Then the purified mRNA samples were fragmented, and cDNA samples were synthesised by reverse transcription to complete library construction.

After finishing the library preparation, a step of library quality control was performed. The libraries were checked with Qubit and real-time PCR for quantification and bioanalyzer for size distribution test. Only quantified libraries were pooled and sequenced by using Illumina NovaSeq platform to generate paired-end reads of 150 bp length.

2.4. Bioinformatic analysis

Bioinformatic analysis of the RNA-Seq data was carried out, following the steps: data quality control, mapping to reference genome, gene expression quantification, differential expression analysis, and enrichment analysis.

2.4.1. Data quality control

Data quality control of raw data (raw reads) was carried out before bioinformatics analysis. Raw reads were inputted to fastp software (Chen et al., 2018), which obtained clean reads from the raw reads and removed reads containing adapter, undefined reads, and reads of low quality. Meanwhile, two sequencing quality scores, Q20 and Q30, which represent for a probability of incorrect base calling of 1 in 100 (99 %), and 1 in 1000 (99.9 %), respectively, as well as GC content of the clean reads were calculated.

2.4.2. Mapping to reference genome

Then the clean reads were aligned to human reference genome, and the reads numbers mapped to each gene were counted. Gene expression quantification was estimated based on the count of sequencing mapped to the genome, because the number of read counts is proportional to gene expression level.

2.4.3. Quantification of gene expression level

Gene expression levels were normalized by using FPKM (Fragments Per Kilobase of transcript per Million base pairs sequenced) method, which is a normalization method based on gene length and sequencing depth [34]. Total counts in a sample were added up and divided by 1, 000,000 (per million) as a scale factor. Then the counts for each gene in the sample were divided by the scaling factor, which was normalized to sequencing depth. Followed divided by the gene length to get FPKM.

2.4.4. Differential expression analysis

Differentially expressed genes were determined by using DESeq2 software [35], which differentiate differentially expressed genes (DEGs) based on the raw count numbers. DESeq2 automatically performs a normalization based on built-in standardization algorithm where geometric mean of raw counts of each gene across all samples is calculated. The raw counts for a gene in each sample is divided by the geometric mean. The median of these ratios in a sample is the size factor for the sample. Finally, raw counts of each gene in each sample were normalized by the size factor (median ratio). Besides, DESeq2 used a model based on negative binomial distribution for significant test. In addition, adjusted p value (padj) was calculated based on Benjamini and Hochberg's method to control for false discovery rate [36]. Genes in agreement with the screening threshold, $|\log2(\text{FoldChange})| \geq 1$ and padj ≤ 0.05, were assigned as significant DEGs.

2.4.5. Enrichment analysis of differentially expressed genes

Kyoto Encyclopedia of Genes and Genomes (KEGG) enrichment, and DisGeNET enrichment of the differentially expressed genes were performed by a clusterProfiler R package. Padj smaller than 0.05 was considered as significantly enriched by the differentially expressed genes.

2.5. DNA methylation analysis

2.5.1. DNA extraction

DNA from HHL-16 cells was extracted by using DNA Mini Kit. Cells were collected as the procedures described in previous study [37]. The cell pellet was resuspended with 200 μl PBS. Then, 20 μl proteinase K and 200 μl Buffer AL was added into the cell pellet. After vortex for 30 s, the samples were incubated in a heat block at 56 °C for 10 min 200 μl absolute ethanol was added into the samples and mixed well by vortex. The mixture was transferred to the Mini spin column placed in a 2 ml collection tube and centrifuged at 8000 rpm for 1 min. After discarding the solution in the collection tube, 500 μl Buffer AW1 was added into the Mini spin column and centrifuged at 8000 rpm for 1 min. Then 500 μl Buffer AW2 was added and centrifuged at 14000 rpm for 3 min. The Mini spin column was placed in a new 2 ml collection tube and centrifuged at 14000 rpm for 1 min to dry the column membrane. Finally, the Mini spin column was placed in a new 1.5 ml nuclease-free microtube and added with nuclease-free water, and DNA samples were eluted and collected after a centrifuge at 8000 rpm for 1 min. The quality and concentrations of DNA samples were quantified by NanoDrop ND-100 Spectrophotometer. Purified DNA samples were kept in −20 °C for further analysis.

2.5.2. DNA methylation sequencing

DNA methylation analysis at the promoter regions of interested genes was performed by the Genome Centre, Barts and The London, Queen Mary University of London, after receiving the extracted DNA samples by our lab. The DNA samples were tested for a quality control, and only those that passed the test were used for the next step. Primer pairs were designed to cover the areas of interest genes. After PCR optimization of the primer pairs, bisulfite conversion of controls and samples were performed. Then samples were amplified by PCR, and the products were pooled and cleaned after a gel electrophoresis, then the samples were barcoded. The barcoded samples were diluted to 4.1 nM and loaded onto MiSeq for sequencing. Finally, Bismark analysis on raw data was performed to get methylation levels of specific loci. A report of methylation levels of each specific loci was provided by the Genome Centre, Barts and The London, Queen Mary University of London.

3. Results

3.1. Alignment of sequencing reads

Concentrations and quality of total RNA samples from HHL-16 cells treated with AFB1 and its control group were tested for sample quality control, all the RNA samples passed the sample quality control, having a concentration of at least 200 ng/μl and the best integrity value of 10 (Appendix table and Fig. 1). All RNAs passed these criteria were used for sequencing, and a total of raw reads approximately ranged from 61 million to 81 million 150 bp-paired ends, with high quality metrics

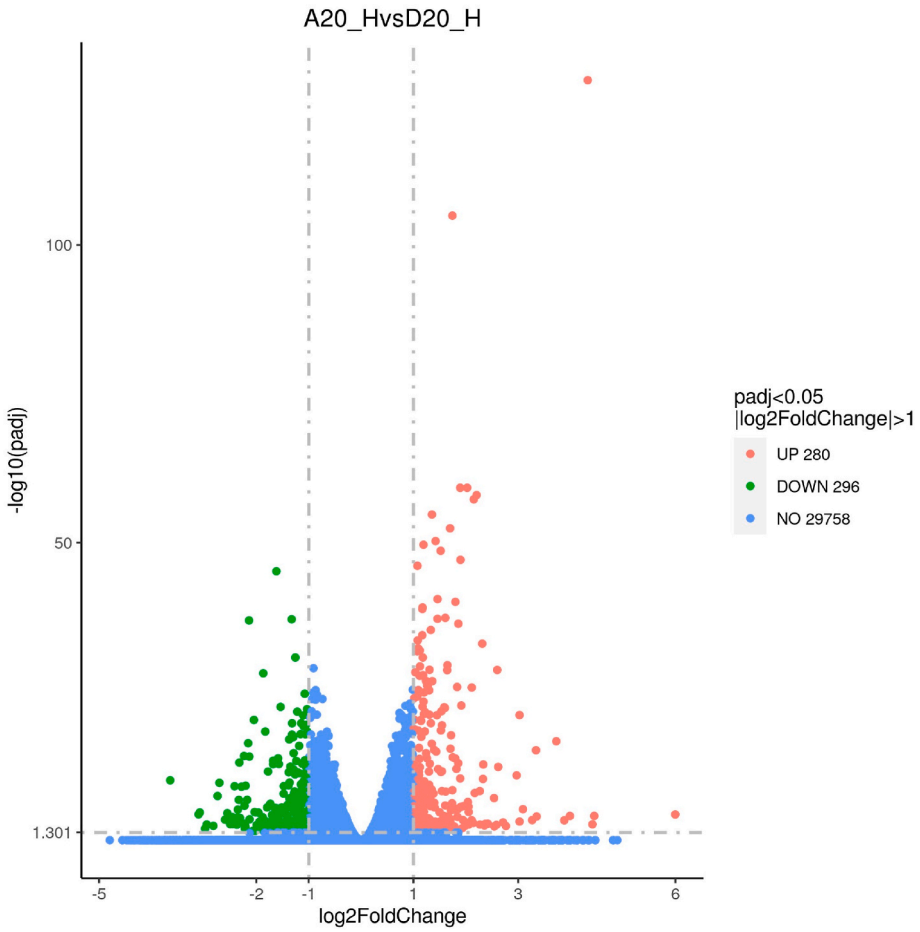

Fig. 1. Volcano map of differentially expressed genes (DEGs) in HHL-16 cells after 20 μg/ml AFB1 treatment for 24 h. A20_H: 20 μg/ml AFB1 treatment in HHL-16 cells; D20_H: 1:1000 diluted DMSO, which is equivalent to the concentration in 20 μg/ml AFB1 treatment; Padj: adjusted p value. Experiment was performed in three biological repeats.

(Q30) were collected. After data filtering of reads with adapter, undetermined reads, and low-quality reads, there were a minimum of 61 million reads in each of the six samples, and over 96 % reads in each sample were successfully mapped after the alignment to human reference genome (Homo sapiens: GRCh38/hg38) (Table 1).

3.2. Differential gene expression analysis

Gene expression levels (FPKM) in each sample were calculated, and correlation analysis and principal component analysis were performed. The results showed that there was a good correlation among the three biological replicates, and the principal component analysis (PCA) plot indicated a clear separation between AFB1 treated group and its control group (Appendix Fig. 2). In the DEGs analysis, the volcano map showed that there were 280 up-regulated and 296 down-regulated genes in HHL-16 cells after 20 μg/ml AFB1 treatment were found (Fig. 1). The 20 most up-regulated and down-regulated genes were summarised (Tables 2 and 3). Noteworthy, four differentially expressed genes (*IL6*, *CCL20*, *BMP2*, and *NDP*) tested under the same conditions as this study found the significant up-regulation of *IL6*, *CCL20*, and *BMP2*, and down-regulation of *NDP* [37], which is consistent with the RNA-Seq results in the study. In the RNA-Seq results, *IL6*, *CCL20*, *BMP2* were also significantly up-regulated in HHL-16 cells after 20 μg/ml AFB1 treatment for 24 h with Log2FoldChange of 1.91, 3.35 and 1.31 (padj = 2.18E-23, 0.0001, and 1.33E-13), respectively, and it was also confirmed that *NDP* was significantly down-regulated with Log2FoldChange of −2.37 (padj = 0.0002). Therefore, the RNA-Seq results are well-validated. Notably, the RNA-Seq data indicated that another gene encoding a CYP enzyme, *CYP1A1*, was also significantly up-regulated (Log2FoldChange = 1.82, padj = 1.00E-12) in HHL-16 cells after the AFB1 treatment.

Table 1
Summary of RNA-Seq datasets in HHL-16 cells.

Sample	Raw reads	Clean reads	Q20	Q30	GC%	Total map (%)
D20_1	62197290	61235132	97.45	92.97	49.76	58871277(96.14)
D20_2	78716718	76914754	97.46	93.04	49.98	74008832(96.22)
D20_3	81508632	80514018	97.59	93.32	49.59	77674229(96.47)
A20_1	81284790	80136996	97.28	92.69	49.83	77047567(96.14)
A20_2	79376720	78113318	97.43	93.02	50.06	75257819(96.34)
A20_3	82993838	81694306	97.59	93.2	49.6	78994023(96.69)

D20: 1 in 1000 diluted DMSO treatment (equivalent to the concentration in 20 μg/ml AFB1 treatment) in HHL-16 cells for 24 h. A20: 20 μg/ml AFB1 treatment.

Table 2
Summary of 20 the most up-regulated genes in HHL-16 cells after 20 μg/ml AFB1 treatment for 24 h.

No.	Gene name	Log2FoldChange	Padj	Gene description 1
1	CALCA	6.00	4.69E-05	Calcitonin related polypeptide alpha
2	TUBB2BP1	4.45	8.36E-05	Tubulin beta 2B class IIb pseudogene 1
3	AC022217.2	4.42	0.002	Novel transcript
4	IL24	4.33	2.14E-128	Interleukin 24
5	RHCG	3.99	8.45E-05	Rh family C glycoprotein
6	AC022217.1	3.88	0.0005	Family with sequence similarity 58, member A (FAM58A) pseudogene
7	C11orf96	3.73	2.22E-17	Chromosome 11 open reading frame 96
8	CCL20	3.35	0.0001	C–C motif chemokine ligand 20
9	CXCL8	3.34	7.23E-16	C-X-C motif chemokine ligand 8
10	AL596223.1	3.27	0.0004	Uncharacterized LOC101928994
11	ARC	3.09	6.17E-06	Activity regulated cytoskeleton associated protein
12	NPPC	3.02	0.0007	Natriuretic peptide C
13	HAP1	3.02	8.97E-22	Huntingtin associated protein 1
14	DMBT1	2.97	1.22E-11	Deleted in malignant brain tumors 1
15	AC003092.1	2.77	0.004	Novel transcript
16	SPINK1	2.71	0.001	Serine peptidase inhibitor, Kazal type 1
17	NR4A3	2.62	4.64E-13	Nuclear receptor subfamily 4 group A member 3
18	UBE2QL1	2.60	2.39E-29	Ubiquitin conjugating enzyme E2 Q family like 1
19	ZNF341-AS1	2.58	0.003	ZNF341 antisense RNA 1
20	IL1RL1	2.54	0.005	interleukin 1 receptor like 1

3.3. KEGG enrichment analysis of the differentially expressed genes

To find the significantly enriched pathways related to the DEGs, KEGG enrichment analysis was carried out. The top 20 enriched KEGG pathways were selected as shown in Fig. 2. The KEGG enrichment analysis indicated that 7 pathways were significantly enriched, including cytokine-cytokine receptor interaction, NF-kappa B signalling pathway, TNF signalling pathway, IL-17 signalling pathway, amoebiasis, MAPK signalling pathway, and lipid and atherosclerosis (Fig. 2). The detailed information of significant levels, up-regulated, and down-regulated genes involved in the 7 significantly enriched pathways was summarised (Table 4).

3.4. DisGeNET enrichment analysis of the differentially expressed genes

Significantly associated human diseases to the DEGs in HHL-16 cells in response to the AFB1 treatment were also discovered by using the DisGeNET database. In total, 47 significantly enriched terms of human diseases were found, 20 of the most significantly enriched diseases were displayed in the figure (Fig. 3). The results indicated that the most associated diseases included inflammation, some types of vascular diseases (i.e. myocardial ischemia), musculoskeletal diseases, premature birth, foetal diseases, susceptibility to infection (i.e. helicobacter pylori infection), and cancer (i.e. primary effusion lymphoma).

3.5. DNA methylation analysis of IL6 and CCL20 in HHL-16 cells after single AFB1 treatment

Previous investigation of effects of aflatoxin on gene expression of gene of interests found that aflatoxin caused significantly up-regulation of *IL6* and *CCL20* [37]. To explore whether the gene expression changes of *IL6* and *CCL20* is a cause of DNA methylation, DNA methylation levels at the areas of interest of *IL6* and *CCL20* in HHL-16 cells after 20 μg/ml AFB1 treatment for 24 h, including the promoter regions and parts of the areas near the transcription start site, has been analysed by the Genome Centre, Barts and The London, Queen Mary University of London. Results (Fig. 4) demonstrated that there was significant difference in DNA methylation between position 1–7 and position 8–18 in *IL6* in HHL-16 cells, but there is no significant difference of each CpG sites after 20 μg/ml AFB1 treatment for 24 h compared to the control group (D20 treatment).

With respect to the methylation levels in *CCL20*, 21 CpG sites were analysed within the promoter regions and parts areas around its transcription start site. As the results (Fig. 5) indicated that there was variation of methylation levels across the CpG sites, and there was a decreased methylation level in position 21 after AFB1 treatment compared to the control treatment (D20). Due to methylation levels in two replicates not determined in position 21 in the DMSO treatment, it was not possible to perform a statistical difference analysis between AFB1 treatment. However, because there is no difference between untreated cells and the DMSO treatment (Appendix Fig. 3), an imputed

Table 3
Summary of 20 the most down-regulated genes in HHL-16 cells after 20 μg/ml AFB1 treatment for 24 h.

No.	Gene name	Log2FoldChange	Padj	Gene description 1
1	NLGN1	−3.64	8.36E-11	Neuroligin 1
2	LINGO2	−3.10	4.48E-05	Leucine rich repeat and Ig domain containing 2
3	AC110373.1	−3.08	2.19E-05	Glycerol kinase 2 pseudogene
4	BMS1P7	−2.98	0.01	BMS1, ribosome biogenesis factor pseudogene 7
5	BNC2-AS1	−2.95	0.002	BNC2 antisense RNA 1
6	TMEM178B	−2.82	0.003	Transmembrane protein 178B
7	GRIP1	−2.74	3.69E-08	Glutamate receptor interacting protein 1
8	PAPPA2	−2.70	2.20E-10	Pappalysin 2
9	KCNIP1	−2.60	0.0004	Potassium voltage-gated channel interacting protein 1
10	PDGFD	−2.55	2.92E-05	Platelet derived growth factor D
11	PRKCQ	−2.50	0.002	Protein kinase C theta
12	EDN2	−2.49	0.0002	Endothelin 2
13	ENOX1	−2.46	0.0001	Ecto-NOX disulfide-thiol exchanger 1
14	TNFSF18	−2.45	0.0006	TNF superfamily member 18
15	PCDHB13	−2.45	0.002	Protocadherin beta 13
16	PCDH18	−2.45	0.0003	Protocadherin 18
17	MDGA2	−2.41	8.19E-10	MAM domain containing glycosylphosphatidylinositol anchor 2
18	GNG7	−2.40	0.0003	G protein subunit gamma 7
19	PCDHB14	−2.37	0.003	Protocadherin beta 14
20	NDP	−2.36	0.0002	Norrin cystine knot growth factor

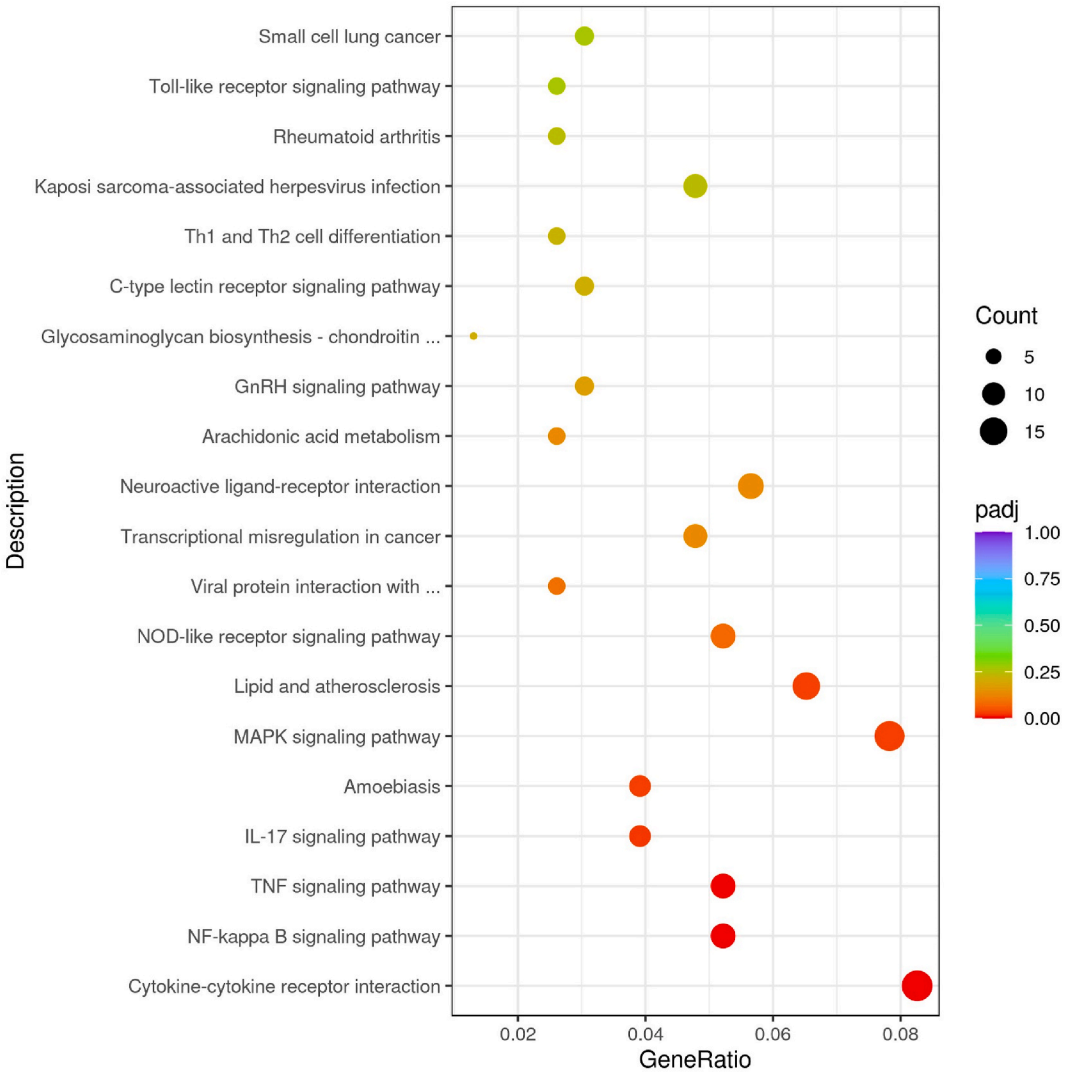

Fig. 2. Scatter plot of KEGG enrichment analysis of the differentially expressed genes in HHL-16 cells in response to the AFB1 treatment. The size of a point represents the gene numbers that annotated to the specific KEGG pathway. The colour from purple to red represents the significant levels of enriched pathways. (For interpretation of the references to colour in this figure legend, the reader is referred to the Web version of this article.)

mean value for the DMSO treatment was calculated based on the addition of the methylation levels in position 21 from the untreated cells and the DMSO treatment. Then a statistical comparison to AFB1 treatment was performed based on the imputed data. The results showed that it was a significant decrease of methylation level at position 21 after 20 μg/ml AFB1 treatment on HHL-16 cells for 24 h ($p = 0.02$) (Fig. 5).

4. Discussion

In this study, we have characterised the transcriptome profile of HHL-16 cells in response to AFB1 treatment, and the main findings of the study were: 1) 576 significant DEGs were found in HHL-16 cells after 20 μg/ml AFB1 treatment for 24 h; 2) seven significantly enriched pathways associated to the DEGs were discovered, including cytokine-cytokine receptor interaction, NF-kappa B signalling pathway, TNF signalling pathway, IL-17 signalling pathway, amoebiasis, MAPK signalling pathway, and lipid and atherosclerosis; 3) significantly enriched human diseases related to the DEGs consisted of the examples of inflammation, early development disease, and cancer. Therefore, we concluded that AFB1 modulates the expression of genes related to the pathways that have crucial roles in inflammatory response, growth, and cancers. Transcriptome analysis in a tumorigenic cell line, HepG2, also found TNF and NF-kB signalling pathways affected by AFB1 treatment at similar concentrations as used in our study [38], however, additional DNA repair pathways were also induced in HepG2 cells, which we did not observe in the HHL-16 cells. The difference may be that HHL-16 cells are less sensitive to AFB1 than HepG2 cells [37], and it may require longer exposure time or higher concentrations of AFB1 treatment to initiate the process.

To our knowledge, there is limited reporting of the transcriptome changes in a non-tumorigenic hepatocyte cell line in response to AFB1. Compared to traditional microarray-based methods, RNA-Seq has several advantages on the analysis of transcriptome changes, which are that it is more quantitatively accurate, has much lower limit of detection, and the ability to detect novel transcripts [39,40]. AFB1 is known as a mutagenic and genotoxic mycotoxin, and its DNA damage characteristic have been broadly reported in various studies [41–43]. Here we also found a significant induction of several genes encoding DNA damage inducible transcripts, e.g., DNA damage-inducible transcript 3 (DDIT3) and growth arrest and DNA damage-inducible alpha (GADD45A), with log2FoldChange of 1.89 (padj = 5.96E-60) and 1.9 (padj = 7.58E-48), respectively. However, no significant induction of DNA repair genes was observed, which might be related to the exposure time or concentration to AFB1 not reaching a threshold for this. Apart

Table 4
Summary of significant levels, up-regulated and down-regulated genes in the significantly enriched pathways from KEGG analysis.

Significantly enriched pathways	Padj	Up-regulated genes	Down-regulated genes
Cytokine-cytokine receptor interaction	0.0003	IL24, IL11, IL6, LIF, CXCL8, BMP2, CXCL2, TNFSF15, NGFR, CXCL3, IL1RN, IL10RA, IL1RL1, TNFRSF9, CSF2	INHBB, IL17RE, TNFSF18, TNFSF4
NF-kappa B signalling pathway	0.0007	RELB, GADD45A, NFKB2, TNFAIP3, TRAF1, BIRC3, CXCL8, CXCL2, PTGS2, CXCL3	PRKCQ, CD14
TNF signalling pathway	0.005	TNFAIP3, IRF1, IL6, TRAF1, LIF, BIRC3, CXCL2, PTGS2, CXCL3, CSF2	MAP2K6, MAPK10
IL-17 signaling pathway	0.02	TNFAIP3, IL6, CXCL8, CXCL2, PTGS2, CXCL3, CSF2	IL17RE, MAPK10
Amoebiasis	0.02	TNFAIP3, IL6, CXCL8, CXCL2, PTGS2, CXCL3, CSF2	PLCB4, COL1A1, LAMA2, CD14
MAPK signalling pathway	0.02	DDIT3, RELB, GADD45A, NFKB2, AREG, PLA2G4C, DUSP2, NGFR, SCAT8, DUSP5, HSPA6, MAPK8IP2	PDGFD, CACNG4, MAP2K6, CD14, DUSP9, MAPK10
Lipid and atherosclerosis	0.03	DDIT3, ERN1, IL6, CXCL8, IRF7, CYP1A1, CXCL2, CXCL3, HSPA6,	PLCB4, CAMK2A, MAP2K6, CD14, MAPK10

from the annotated transcripts, some novel transcripts were found in HHL-16 cells after 20 μg/ml AFB1 treatment for 24 h, such as: AC245041.2, AC007249.1, and AC007249.2, etc. Additionally, 576 significantly DEGs were found, and the differentially expressed patterns of the four DEGs (*IL6*, *CCL20*, *BMP2*, and *NDP*) measured by RT-qPCR in a recent study [37], are consistent with the results measured by RNA-Seq method, indicating the RNA-Seq results are reliable and reproducible. Therefore, to ensure a consistent result of gene expression, it is important to use separate RT-qPCR to validate RNA-Seq results, which has been an empirical practice that widely adopted in various RNA-Seq studies [31,44–46].

In KEGG enrichment analysis of DEGs in HHL-16 cells after the AFB1 treatment, the most significantly enriched pathways were cytokine-cytokine receptor interaction, NF-kappa B signalling pathway, and TNF signalling pathway. The set of DEGs were most significantly involved in cytokine-related pathway, such as: up-regulation of *IL24*, *IL11*, *IL6*, *LIF*, *CXCL8* and *IL1R*, and down-regulation of *INHBB*, *IL17*RE, *TNFSF18*, and *TNFSF4*. An imbalanced expression of cytokines was extensively reported in immune-related organs of animals or cell lines in response to AFB1, which indicated an inflammatory response and affected immune function [47–51]. Therefore, in view of the interference of cytokine expression in HHL-16 cells caused by AFB1, it is possible that an inflammatory response could be activated in response to the stimulus of AFB1.

In this study, DEGs enriched in NF-kB pathway included upregulation of *RELB*, *NFKB2*, *GADD45A*, *TNFAIP3*, and *BIRC3*, among others, and downregulation of *PRKCD* and *CD14*. NF-kB pathway is a well-known pathway implicated in various cancers [52–54], which might be because of the involvement of many transcription factors in the pathway that can be commonly induced by different cellular stimulus to regulate immune and inflammatory response to protect cells from apoptosis [55,56]. Evidence indicated that NF-kB can be activated both by pro-inflammatory cytokines and members of TNF signalling pathway [57]. Excessive production of IL-17A, IL-21, IL-22, TNF-α, and IL-6 were observed in colorectal cancers in mice, and this was associated with increased activation of STAT3/NF-kB pathway [58]. Therefore, we propose up-regulation of several pro-inflammatory cytokines, such as IL6, may activate the NF-kB pathway. Evidence has also indicated that IL6 can form a feedback loop where NF-kB activation leads to the induction of IL6, and further enhancing NF-kB activity [59]. Therefore, more investigations are warranted to elucidate the underlying mechanisms. In the TNF signalling pathways, up-regulated genes including TNFAIP3, IRF1 and TRAF1, were observed in the present study. It was evident that TNFAIP3 is an inhibitor of NF-kB pathway [60,61], while stimulatory effect of TRAF1 on NF-kB was found [62]. Taken together, the evidence implies a dynamic modulation in terms of NF-kB pathway.

In normal cells, NF-kB becomes transiently activated in response to cellular stimuli, subsequently returning to the inactive state [56]. However, in tumour cells, multiple mechanisms may cause impaired modulation of NF-kB, leading to a continuous activation of the pathway, which facilitates the proliferation and progression of tumour cells [63,64]. Therefore, in this study, according to the affected pathways: cytokine-related, TNF, and NF-kB pathways in HHL-16 cells by AFB1, together with previous evidence mentioned above, the mechanism we propose is that AFB1 can cause an inflammatory response, which might further activate NF-kB to regulate genes in response to the stress caused by AFB1. Meanwhile, TNF signalling pathway has duplex modulation of NF-kB activation via both enhancing activation and suppressing activation. Once the modulation balance of NF-kB is disrupted in the long term under the effects of consistent stimulation of AFB1, eventually the cells will be driven to an unlimited proliferation and progression to cancer.

In addition, evidence indicated that chronic inflammation was linked to growth impairment by causing disruption of GH-IGF1 axis as well as the link to insulin resistance [65]. Over-expressed IL6 in transgenic mice showed chronic inflammation, which was associated with decreased IGF1 level in serum and caused growth impairment [66]. However, in HHL-16 cells, we did not observe differentially expressed genes in the GH-IGF1 axis. After a deep investigation into RNA-Seq data of gene expression levels (FPKM) of GH-IGF1 axis, we found that genes involved in the GH-IGF1 axis including *GH1*, *GH2*, *GHR*, *IGF1*, and *IGF2* were not expressed in HHL-16 cells, which limited investigation of whether increased IL6 lead to abnormalities to GH-IGF axis in the cells after AFB1 treatment. Generally, IGF1 is predominantly produced by the liver [67]. One reason for the absence of GH-IGF1 axis in HHL-16 cells may be because the expression of genes in the axis was altered when the cell line was immortalised. A previous study assessing aflatoxin exposure levels in Kenyan schoolchildren indicated that there was a negative correlation between aflatoxin exposure level and protein levels of IGF1 and IGFBP3, with a path analysis demonstrating that lower expression of IGF1 contributed to 16 % of the effects of aflatoxin exposure on child height [25]. Therefore, the effects of IL6 on the GH-IGF1 axis are worthy of investigation in other cell lines or animal models exposed to aflatoxin.

We found a significant difference of decreased DNA methylation at a CpG site near the transcription start site of *CCL20* in HHL-16 cells after AFB1 treatment compared to the control group, which might be responsible for the up-regulation of *CCL20*. *CCL20* has previously been reported to be upregulated in response to AFB1 exposure [68]. There is evidence reported that in the liver, *CCL20* can exacerbate AFB1-induced hepatotoxicity by contributing to inflammatory response, as well as lead to increased liver damage [69]. Elevated *CCL20* has been associated with promoter hypomethylation in esophageal cancer [70]. Recently, promoter hypomethylation of *CCL20* causing increased mRNA level of *CCL20* was also indicated in esophageal adenocarcinoma, and the methylation pattern was correlated with esophageal status, which suggested that *CCL20* could be a novel biomarker for early detection of esophageal cancer [71]. Therefore, the hypomethylation change and overexpression of *CCL20* observed in HHL-16 cells after AFB1 treatment strengthen the evidence of aflatoxin-caused DNA methylation. More DNA methylation analysis on *CCL20* in other cell lines treated with AFB1 as well as in animals or populations with AFB1 exposure are required for further validation.

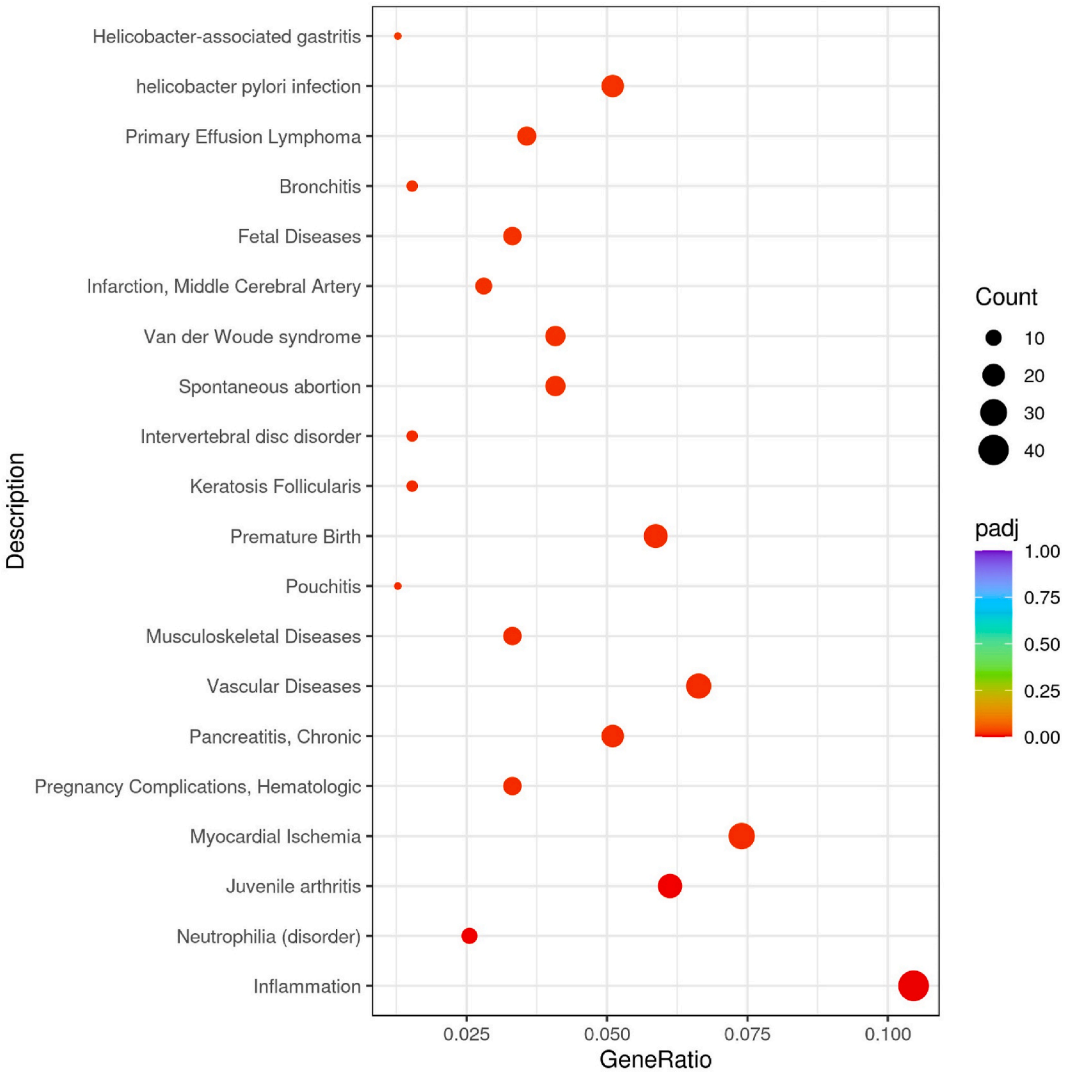

Fig. 3. Scatter plot of DisGeNET enrichment analysis of the differentially expressed genes in HHL-16 cells in response to the AFB1 treatment. The top 20 significantly enriched human diseases terms associated to the DEGs were displayed. The size of a point represents the gene numbers that annotated to the specific human disease. The colour from purple to red represents the significant levels of the enrichment. (For interpretation of the references to colour in this figure legend, the reader is referred to the Web version of this article.)

5. Conclusions

In summary, in AFB1 treated HHL-16 cells, over 500 DEGs were found, and the most significantly involved pathways of the DEGs were cytokine-related, TNF, and NF-kB pathways. Therefore, we hypothesize that AFB1 modulates the expression of gene sets implicated in inflammation, growth factor pathways, and cancer, through the interactions among cytokine-related/TNF/NF-kB pathways. The effects of aflatoxin on gene expression and DNA methylation are potential mechanisms responsible for aflatoxin health effects.

CRediT authorship contribution statement

Hang Wu: Writing – review & editing, Writing – original draft, Visualization, Methodology, Formal analysis, Data curation, Conceptualization. **Yun Yun Gong:** Writing – review & editing, Supervision, Conceptualization. **John Huntriss:** Writing – review & editing, Supervision, Methodology, Conceptualization. **Michael N. Routledge:** Writing – review & editing, Supervision, Conceptualization.

Informed consent statement

Not applicable.

Data availability statement

The data presented in this study are available on request from the corresponding author.

Funding

This research was supported by China Scholarship Council and University of Leeds.

Declaration of competing interest

The authors declare that they have no known competing financial interests or personal relationships that could have appeared to influence the work reported in this paper.

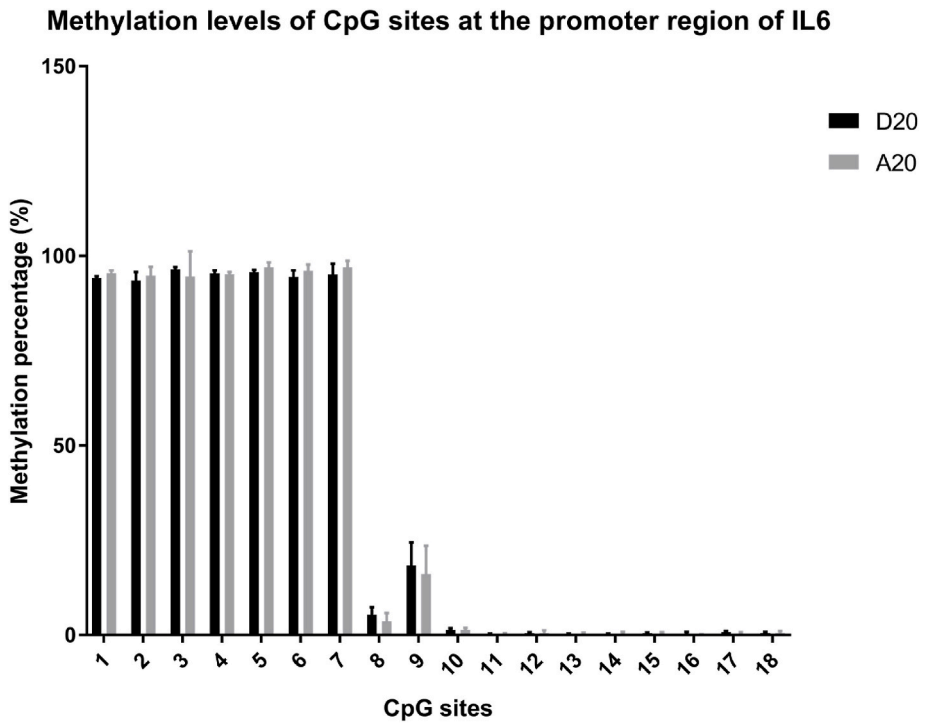

Fig. 4. DNA methylation analysis at promoter regions of *IL6* in HHL-16 cells after 20 μg/ml AFB1 treatment for 24 h. D20: 1:1000 diluted DMSO, which is equivalent to the concentration in 20 μg/ml AFB1 treatment. A20: AFB1 treatment. The DNA methylation levels of 18 CpG sites were analysed in the *IL6* promoter in total. Data presented as mean ± SD with three biological replicates.

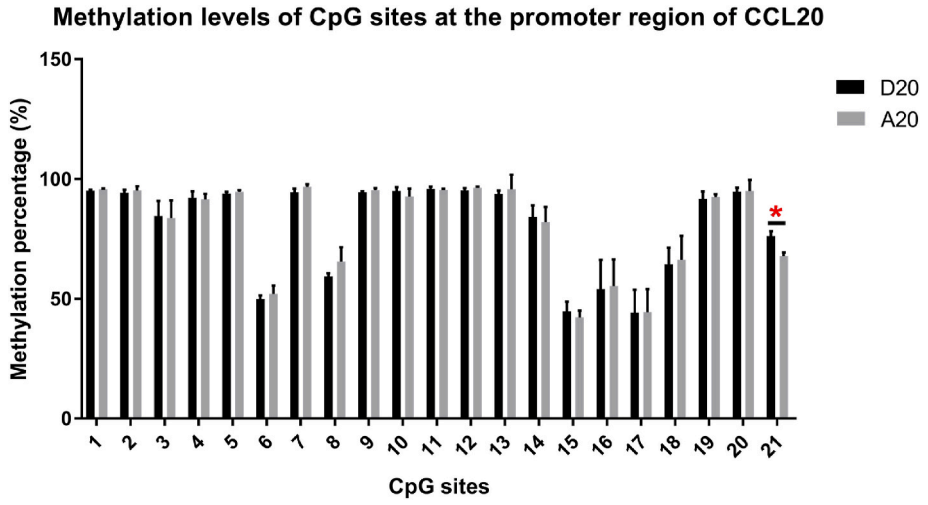

Fig. 5. DNA methylation analysis at the promoter region of *CCL20* in HHL-16 cells after 20 μg/ml AFB1 treatment for 24 h. D20: 1:1000 diluted DMSO, which is equivalent to the concentration in 20 μg/ml AFB1 treatment. A20: AFB1 treatment. Totally, DNA methylation levels of 21 CpG sites around the promoter regions of *CCL20* were analysed. Data presented as mean ± SD with three biological replicates.

Appendix A. Supplementary data

Supplementary data to this article can be found online at https://doi.org/10.1016/j.cbi.2025.111531.

Data availability

Data will be made available on request.

References

[1] C.P. Wild, Y.Y. Gong, Mycotoxins and human disease: a largely ignored global health issue, Carcinogenesis 31 (2010) 71–82.
[2] D. Dhanasekaran, S. Shanmugapriya, N. Thajuddin, A. Panneerselvam, Aflatoxins and aflatoxicosis in human and animals, Aflatoxins-Biochemistry, Mol. Biol. 10 (2011) 221–254.
[3] Y.Y. Gong, S. Watson, M.N. Routledge, Aflatoxin exposure and associated human health effects, a review of epidemiological studies, Food Saf 4 (2016) 14–27, https://doi.org/10.14252/foodsafetyfscj.2015026.
[4] V. Ostry, F. Malir, J. Toman, Y. Grosse, Mycotoxins as human carcinogens—the IARC Monographs classification, Mycotoxin Res. 33 (2017) 65–73.
[5] Y. Liu, C.-C.H. Chang, G.M. Marsh, F. Wu, Population attributable risk of aflatoxin-related liver cancer: systematic review and meta-analysis, Eur. J. Cancer 48 (2012) 2125–2136.

[6] A. Ngindu, P. Kenya, D. Ocheng, T. Omondi, W. Ngare, D. Gatei, B. Johnson, J. Ngira, H. Nandwa, A. Jansen, Outbreak of acute hepatitis caused by aflatoxin poisoning in Kenya, Lancet 319 (1982) 1346–1348.
[7] CDC, Outbreak of aflatoxin poisoning–eastern and central provinces, Kenya, January-July 2004, MMWR Morb. Mortal. Wkly. Rep. 53 (2004) 790–793.
[8] L. Unnevehr, D. Grace, Aflatoxins: finding solutions for improved food safety, Intl. Food Policy Res. Inst. (2013).
[9] Y. Jiang, P.E. Jolly, P. Preko, J.-S. Wang, W.O. Ellis, T.D. Phillips, J.H. Williams, Aflatoxin-related immune dysfunction in health and in human immunodeficiency virus disease, Clin. Dev. Immunol. 2008 (2008).
[10] P. Khlangwiset, G.S. Shephard, F. Wu, Aflatoxins and growth impairment: a review, Crit. Rev. Toxicol. 41 (2011) 740–755.
[11] B. Bressac, M. Kew, J. Wands, M. Ozturk, Selective G to T mutations of p53 gene in hepatocellular carcinoma from southern Africa, Nature 350 (1991) 429–431.
[12] I.C. Hsu, R.A. Metcalf, T. Sun, J.A. Welsh, N.J. Wang, C.C. Harris, Mutational hot spot in the p53 gene in human hepatocellular carcinomas, Nature 350 (1991) 427–428.
[13] F. Aguilar, S.P. Hussain, P. Cerutti, Aflatoxin B1 induces the transversion of G–> T in codon 249 of the p53 tumor suppressor gene in human hepatocytes, Proc. Natl. Acad. Sci. 90 (1993) 8586–8590.
[14] E.A. Bailey, R.S. Iyer, M.P. Stone, T.M. Harris, J.M. Essigmann, Mutational properties of the primary aflatoxin B1-DNA adduct, Proc. Natl. Acad. Sci. 93 (1996) 1535–1539.
[15] K. Mace, F. Aguilar, J.-S. Wang, P. Vautravers, M. Gomez-Lechon, F.J. Gonzalez, J. Groopman, C.C. Harris, A.M. Pfeifer, Aflatoxin B1-induced DNA adduct formation and p53 mutations in CYP450-expressing human liver cell lines, Carcinogenesis 18 (1997) 1291–1297.
[16] G.Y. Michael, P. Thaxton, P.B. Hamilton, Impairment of the reticuloendothelial system of chickens during aflatoxicosis, Poult. Sci. 52 (1973) 1206–1207.
[17] M.S. Mohsenzadeh, N. Hedayati, B. Riahi-Zanjani, G. Karimi, Immunosuppression following dietary aflatoxin B1 exposure: a review of the existing evidence, Toxin Rev. 35 (2016) 121–127.
[18] Y.-H. Cheng, T.-F. Shen, V.F. Pang, B.-J. Chen, Effects of aflatoxin and carotenoids on growth performance and immune response in mule ducklings, Comp. Biochem. Physiol., Part C: Toxicol. Pharmacol. 128 (2001) 19–26.
[19] H. Oguz, H.H. Hadimli, V. Kurtoglu, O. Erganis, Evaluation of humoral immunity of broilers during chronic aflatoxin (50 and 100 ppb) and clinoptilolite exposure, Rev. Med. Vet. 154 (2003) 483–486.
[20] C.E.P. Zimmermann, A.K. Machado, F.C. Cadoná, J.A.S. Jaques, K.B. Schlemmer, C. Lautert, I.B.M. Cruz, R.A. Zanette, D.B.R. Leal, J.M. Santurio, In-vitro cytotoxicity of aflatoxin B1 to broiler lymphocytes of broiler chickens, Brazilian J. Poult. Sci. 16 (2014) 307–312.
[21] Y.Y. Gong, A. Hounsa, S. Egal, P.C. Turner, A.E. Sutcliffe, A.J. Hall, K. Cardwell, C. P. Wild, Postweaning exposure to aflatoxin results in impaired child growth: a longitudinal study in Benin, West Africa, Environ. Health Perspect. 112 (2004) 1334–1338.
[22] G.M. Kiarie, P. Dominguez-Salas, S.K. Kang'ethe, D. Grace, J. Lindahl, Aflatoxin exposure among young children in urban low-income areas of Nairobi and association with child growth, Afr. J. Food Nutr. Sci. 16 (2016) 10967–10990.
[23] Y.Y. Gong, P.C. Turner, A.J. Hall, C.P. Wild, Aflatoxin exposure and impaired child growth in West Africa: an unexplored international public health burden?, in: Mycotoxins Detect. Methods, Manag. Public Heal. Agric. Trade Cabi, Wallingford UK, 2008, pp. 53–65.
[24] Y. Gao, X. Bao, L. Meng, H. Liu, J. Wang, N. Zheng, Aflatoxin B1 and aflatoxin M1 induce compromised intestinal integrity through clathrin-mediated endocytosis, Toxins 13 (2021) 184.
[25] J.M. Castelino, M.N. Routledge, S. Wilson, D.W. Dunne, J.K. Mwatha, K. Gachuhi, C.P. Wild, Y.Y. Gong, Aflatoxin exposure is inversely associated with IGF1 and IGFBP3 levels in vitro and in Kenyan schoolchildren, Mol. Nutr. Food Res. 59 (2015) 574–581.
[26] S. Watson, S.E. Moore, M.K. Darboe, G. Chen, Y.-K. Tu, Y.-T. Huang, K.G. Eriksen, R.M. Bernstein, A.M. Prentice, C.P. Wild, Impaired growth in rural Gambian infants exposed to aflatoxin: a prospective cohort study, BMC Public Health 18 (2018) 1247.
[27] H. Hernandez-Vargas, J. Castelino, M.J. Silver, P. Dominguez-Salas, M.-P. Cros, G. Durand, F. Le Calvez-Kelm, A.M. Prentice, C.P. Wild, S.E. Moore, B.J. Henning, Z. Herceg, Y.Y. Gong, M.N. Routledge, Exposure to aflatoxin B1 in utero is associated with DNA methylation in white blood cells of infants in the Gambia, Int. J. Epidemiol. 44 (2015) 1238–1248.
[28] Z. Wang, M. Gerstein, M. Snyder, RNA-Seq: a revolutionary tool for transcriptomics, Nat. Rev. Genet. 10 (2009) 57–63.
[29] N.-Y. Zhang, M. Qi, X. Gao, L. Zhao, J. Liu, C.-Q. Gu, W.-J. Song, C.S. Krumm, L.-H. Sun, D.-S. Qi, Response of the hepatic transcriptome to aflatoxin B1 in ducklings, Toxicon 111 (2016) 69–76.
[30] M.S. Monson, C.J. Cardona, R.A. Coulombe, K.M. Reed, Hepatic transcriptome responses of domesticated and wild Turkey embryos to aflatoxin B1, Toxins 8 (2016) 16.
[31] J. Ma, Y. Liu, Y. Guo, Q. Ma, C. Ji, L. Zhao, Transcriptional profiling of aflatoxin B1-induced oxidative stress and inflammatory response in macrophages, Toxins 13 (2021) 401.
[32] K. Wu, S. Jia, J. Zhang, C. Zhang, S. Wang, S.A. Rajput, L. Sun, D. Qi, Transcriptomics and flow cytometry reveals the cytotoxicity of aflatoxin B1 and aflatoxin M1 in bovine mammary epithelial cells, Ecotoxicol. Environ. Saf. 209 (2021) 111823.
[33] R.F. Clayton, A. Rinaldi, E.E. Kandyba, M. Edward, C. Willberg, P. Klenerman, A. H. Patel, Liver cell lines for the study of hepatocyte functions and immunological response, Liver Int. 25 (2005) 389–402.
[34] A. Mortazavi, B.A. Williams, K. McCue, L. Schaeffer, B. Wold, Mapping and quantifying mammalian transcriptomes by RNA-Seq, Nat. Methods 5 (2008) 621–628.
[35] M.I. Love, W. Huber, S. Anders, Moderated estimation of fold change and dispersion for RNA-seq data with DESeq2, Genome Biol. 15 (2014) 1–21.
[36] Y. Hochberg, Y. Benjamini, More powerful procedures for multiple significance testing, Stat. Med. 9 (1990) 811–818.
[37] H. Wu, Y. Xu, Y.Y. Gong, J. Huntriss, M.N. Routledge, Effects of aflatoxin and fumonisin on gene expression of growth factors and inflammation-related genes in a human hepatocyte cell line, Mutagenesis (2024) geae005.
[38] X. Chen, M.F. Abdallah, C. Grootaert, F. Van Nieuwerburgh, A. Rajkovic, New insights into the combined toxicity of aflatoxin B1 and fumonisin B1 in HepG2 cells using Seahorse respirometry analysis and RNA transcriptome sequencing, Environ. Int. (2023) 107945.
[39] K.J. Mantione, R.M. Kream, H. Kuzelova, R. Ptacek, J. Raboch, J.M. Samuel, G. B. Stefano, Comparing bioinformatic gene expression profiling methods: microarray and RNA-Seq, Med. Sci. Monit. Basic Res. 20 (2014) 138.
[40] M.F. Rai, E.D. Tycksen, L.J. Sandell, R.H. Brophy, Advantages of RNA-seq compared to RNA microarrays for transcriptome profiling of anterior cruciate ligament tears, J. Orthop. Res. 36 (2018) 484–497.
[41] L.L. Bedard, T.E. Massey, Aflatoxin B1-induced DNA damage and its repair, Cancer Lett. 241 (2006) 174–183.
[42] R.J. Verma, Aflatoxin cause DNA damage, Int. J. Hum. Genet. 4 (2004) 231–236.
[43] J. Zhang, N. Zheng, J. Liu, F.D. Li, S.L. Li, J.Q. Wang, Aflatoxin B1 and aflatoxin M1 induced cytotoxicity and DNA damage in differentiated and undifferentiated Caco-2 cells, Food Chem. Toxicol. 83 (2015) 54–60.
[44] X.-L. Liu, R.-Y. Wu, X.-F. Sun, S.-F. Cheng, R.-Q. Zhang, T.-Y. Zhang, X.-F. Zhang, Y. Zhao, W. Shen, L. Li, Mycotoxin zearalenone exposure impairs genomic stability of swine follicular granulosa cells in vitro, Int. J. Biol. Sci. 14 (2018) 294.
[45] G.-L. Zhang, J.-L. Song, Y. Zhou, R.-Q. Zhang, S.-F. Cheng, X.-F. Sun, G.-Q. Qin, W. Shen, L. Li, Differentiation of sow and mouse ovarian granulosa cells exposed to zearalenone in vitro using RNA-seq gene expression, Toxicol. Appl. Pharmacol. 350 (2018) 78–90.
[46] K.E. Reddy, J. young Jeong, Y. Lee, H.-J. Lee, M.S. Kim, D.-W. Kim, H.J. Jung, C. Choe, Y.K. Oh, S.D. Lee, Deoxynivalenol-and zearalenone-contaminated feeds alter gene expression profiles in the livers of piglets, AJAS (Asian-Australas. J. Anim. Sci.) 31 (2018) 595.
[47] G.M. Meissonnier, P. Pinton, J. Laffitte, A.-M. Cossalter, Y.Y. Gong, C.P. Wild, G. Bertin, P. Galtier, I.P. Oswald, Immunotoxicity of aflatoxin B1: impairment of the cell-mediated response to vaccine antigen and modulation of cytokine expression, Toxicol. Appl. Pharmacol. 231 (2008) 142–149.
[48] J.C. Bruneau, E. Stack, R. O'Kennedy, C.E. Loscher, Aflatoxins B1, B2 and G1 modulate cytokine secretion and cell surface marker expression in J774A. 1 murine macrophages, Toxicol. Vitro 26 (2012) 686–693.
[49] G. Qian, L. Tang, X. Guo, F. Wang, M.E. Massey, J. Su, T.L. Guo, J.H. Williams, T. D. Phillips, J. Wang, Aflatoxin B1 modulates the expression of phenotypic markers and cytokines by splenic lymphocytes of male F344 rats, J. Appl. Toxicol. 34 (2014) 241–249.
[50] M. Jiang, X. Peng, J. Fang, H. Cui, Z. Yu, Z. Chen, Effects of aflatoxin B1 on T-cell subsets and mRNA expression of cytokines in the intestine of broilers, Int. J. Mol. Sci. 16 (2015) 6945–6959.
[51] S. Iori, M. Pauletto, I. Bassan, F. Bonsembiante, M.E. Gelain, A. Bardhi, A. Barbarossa, A. Zaghini, M. Dacasto, M. Giantin, Deepening the whole transcriptomics of bovine liver cells exposed to AFB1: a spotlight on toll-like receptor 2, Toxins 14 (2022) 504.
[52] G.G. Chen, J.F.Y. Lee, S.H. Wang, U.P.F. Chan, P.C. Ip, W.Y. Lau, Apoptosis induced by activation of peroxisome-proliferator activated receptor-gamma is associated with Bcl-2 and Nf-kB in human colon cancer, Life Sci. 70 (2002) 2631–2646.
[53] W. Li, D. Tan, M.J. Zenali, R.E. Brown, Constitutive activation of nuclear factor-kappa B (NF-kB) signaling pathway in fibrolamellar hepatocellular carcinoma, Int. J. Clin. Exp. Pathol. 3 (2010) 238.
[54] P. Hassanzadeh, Colorectal cancer and NF-κB signaling pathway, Gastroenterol. Hepatol. from Bed to Bench 4 (2011) 127.
[55] Y. Yamamoto, R.B. Gaynor, Role of the NF-kB pathway in the pathogenesis of human disease states, Curr. Mol. Med. 1 (2001) 287–296.
[56] X. Dolcet, D. Llobet, J. Pallares, X. Matias-Guiu, NF-kB in development and progression of human cancer, Virchows Arch. 446 (2005) 475–482.
[57] M.R. Zinatizadeh, B. Schock, G.M. Chalbatani, P.K. Zarandi, S.A. Jalali, S.R. Miri, The Nuclear Factor Kappa B (NF-kB) signaling in cancer development and immune diseases, Genes Dis 8 (2021) 287–297.
[58] V. De Simone, E. Franze, G. Ronchetti, A. Colantoni, M.C. Fantini, D. Di Fusco, G. S. Sica, P. Sileri, T.T. MacDonald, F. Pallone, Th17-type cytokines, IL-6 and TNF-α synergistically activate STAT3 and NF-kB to promote colorectal cancer cell growth, Oncogene 34 (2015) 3493–3503.
[59] K.K. Nyati, K. Masuda, M.M.-U. Zaman, P.K. Dubey, D. Millrine, J.P. Chalise, M. Higa, S. Li, D.M. Standley, K. Saito, TLR4-induced NF-κB and MAPK signaling regulate the IL-6 mRNA stabilizing protein Arid5a, Nucleic Acids Res. 45 (2017) 2687–2703.
[60] D.L. Boone, E.E. Turer, E.G. Lee, R.-C. Ahmad, M.T. Wheeler, C. Tsui, P. Hurley, M. Chien, S. Chai, O. Hitotsumatsu, The ubiquitin-modifying enzyme A20 is required for termination of Toll-like receptor responses, Nat. Immunol. 5 (2004) 1052–1060.

[61] T. Schioppa, H.O. Nguyen, L. Tiberio, F. Sozio, C. Gaudenzi, M. Passari, A. Del Prete, D. Bosisio, V. Salvi, Inhibition of class I histone deacetylase activity blocks the induction of TNFAIP3 both directly and indirectly via the suppression of endogenous TNF-α, Int. J. Mol. Sci. 23 (2022) 9752.
[62] L. Cabal-Hierro, M. Rodríguez, N. Artime, J. Iglesias, L. Ugarte, M.A. Prado, P. S. Lazo, TRAF-mediated modulation of NF-kB AND JNK activation by TNFR2, Cell. Signal. 26 (2014) 2658–2666.
[63] M. Kojima, T. Morisaki, N. Sasaki, K. Nakano, R. Mibu, M. Tanaka, M. Katano, Increased nuclear factor-kB activation in human colorectal carcinoma and its correlation with tumor progression, Anticancer Res. 24 (2004) 675–682.
[64] O.O. Ogunwobi, T. Harricharran, J. Huaman, A. Galuza, O. Odumuwagun, Y. Tan, G.X. Ma, M.T. Nguyen, Mechanisms of hepatocellular carcinoma progression, World J. Gastroenterol. 25 (2019) 2279.
[65] F. Cirillo, P. Lazzeroni, C. Catellani, C. Sartori, S. Amarri, M.E. Street, MicroRNAs link chronic inflammation in childhood to growth impairment and insulin-resistance, Cytokine Growth Factor Rev. 39 (2018) 1–18.
[66] F. De Benedetti, T. Alonzi, A. Moretta, D. Lazzaro, P. Costa, V. Poli, A. Martini, G. Ciliberto, E. Fattori, Interleukin 6 causes growth impairment in transgenic mice through a decrease in insulin-like growth factor-I. A model for stunted growth in children with chronic inflammation, J. Clin. Investig. 99 (1997) 643–650.
[67] R.D. Kineman, M. del Rio-Moreno, A. Sarmento-Cabral, Understanding the tissue-specific roles of IGF1/IGF1R in regulating metabolism using the Cre/loxP system, J. Mol. Endocrinol. 61 (2018) T187.
[68] J. Guo, W.-R. Yan, J.-K. Tang, X. Jin, H.-H. Xue, T. Wang, Q.-Y. Sun, Z.-X. Liang, L.-W. Zhang, Dietary phillygenin supplementation ameliorates aflatoxin B1-induced oxidative stress, inflammation, and apoptosis in chicken liver, Ecotoxicol. Environ. Saf. 236 (2022) 113481.
[69] C. Dai, E. Tian, Z. Hao, S. Tang, Z. Wang, G. Sharma, H. Jiang, J. Shen, Aflatoxin B1 toxicity and protective effects of curcumin: molecular mechanisms and clinical implications, Antioxidants 11 (2022) 2031.
[70] H. Nan, L. Zhou, W. Liang, J. Meng, K. Lin, M. Li, J. Hou, L. Wang, Epigenetically associated CCL20 upregulation correlates with esophageal cancer progression and immune disorder, Pathol. Pract 228 (2021) 153683.
[71] A.K. Maity, T.C. Stone, V. Ward, A.P. Webster, Z. Yang, A. Hogan, H. McBain, M. Duku, K.M.A. Ho, P. Wolfson, Novel epigenetic network biomarkers for early detection of esophageal cancer, Clin. Epigenet. 14 (2022) 23.